INHOMOGENEOUS STELLAR MODELS. II. MODELS WITH EXHAUSTED CORES IN GRAVITATIONAL CONTRACTION

A. R. SANDAGE* AND M. SCHWARZSCHILD†
Princeton University Observatory
Received June 28, 1952

ABSTRACT

Seven shell-source models with exhausted, gravitationally contracting cores have been computed in detail. The models form an evolutionary sequence starting from a configuration whose isothermal core contains the Schönberg-Chandrasekhar limitating mass. It is found that, as the cores contract, the envelopes greatly expand. Thus from the initial configuration, which is near the main sequence, the stars evolve rapidly to the right in the H-R diagram, amply covering the giant region. In this evolution the gravitational contraction contributes less than 4 per cent to the total luminosity.

A comparison of this theoretical evolution with the observed H-R diagram for globular clusters appears to explain the sudden turnoff from the main sequence to the giant region at about $M_{\text{bol}} = +3.5$.

I. INTRODUCTION

The identification in 1938 of the source of stellar energy with nuclear processes created the problem of finding equilibrium models for giant stars with the high central temperatures required for the nuclear reactions. In recent years a number of investigations[1] have indicated that the solution probably lies with chemically inhomogeneous models. These investigations have shown that certain types of inhomogeneities do lead to large radii with high central temperatures. The various models proposed have differed in the way the inhomogeneities were introduced, according to a variety of assumptions regarding the degrees of mixing and the evolutionary process involved (nuclear transmutations or accretion).

This paper considers a model whose inhomogeneity arises from the following evolutionary process. An initially homogeneous star with a convective core and radiative envelope (Cowling model) which experiences no mixing between the core and envelope starts exhausting its hydrogen supply in the core. The subsequent early stages of the evolution follow those computed by Schönberg and Chandrasekhar,[2] with the core finally exhausted of hydrogen and therefore isothermal. The nuclear-energy production is then confined to a shell between the exhausted core and the radiative envelope. The assumption of no mixing creates a chemical discontinuity between the core and the shell. When the shell has burned outward until it reaches the Schönberg-Chandrasekhar limit for an isothermal core, a new evolutionary process must take place, which is most likely a gravitational contraction of the core. This paper is concerned with the quasi-equilibrium states through which an unmixed model passes after reaching the Schönberg-Chandrasekhar limit.

The main feature differentiating the present models from earlier ones is the occurrence of an additional energy source by gravitational contraction. The distribution of this energy source throughout the exhausted core has here been treated only approximately (assumption 3 in Sec. II), in accordance with the general result that the details of the energy-source distribution have little effect on the model. However, the total amount of energy released by the contraction of the core has been accounted for explicitly (Sec. III).

* William Charles Peyton Advanced Fellow in Astronomy at Princeton University.

† This research was supported in part by funds of the Eugene Higgins Trust allocated to Princeton University.

[1] See Paper I of this series for references, Oke and Schwarzschild, *Ap. J.*, **116**, 317, 1952.

[2] *Ap. J.*, **96**, 161, 1942.

II. ASSUMPTIONS, DEFINITIONS, AND EQUATIONS

The models here considered consist of a hydrogen-rich envelope in radiative equilibrium and a contracting hydrogen-exhausted core, also in radiative equilibrium.

The following simplifying assumptions have been made in the computations: (1) All the sources for nuclear energy are confined to a shell idealized to an infinitely thin sheet located immediately outside the exhausted core. (2) The temperature at the shell, necessary for the carbon cycle, is 3×10^7 ° K throughout the evolutionary stages considered. (3) The distribution of the gravitational energy source in the core is assumed as $\epsilon =$ Constant, where ϵ is the energy liberated per gram. If L_g is the total flux due to the gravitational source in the core, the flux crossing a shell of radius r within the core is $L(r)$ $L_g M_r / M_1$, where M_1 is the total mass within the core. (4) The evolutionary changes are sufficiently slow that dynamical terms in the equilibrium equations are negligible. (5) The mean molecular weight is discontinuous across the interface between the envelope and the core, with an arbitrary jump of a factor of 2 consistent with the assumed abundances of $X_i = 0$, $Y_i = 0.98$, $Z_i = 0.02$ in the core, and $X_e = 0.596$, $Y_e = 0.384$, and $Z_e = 0.02$ in the envelope. (6) The switch from the Kramers opacity law to electron scattering in the envelope is abrupt and occurs at the same place for stars of different masses. (7) Radiation pressure and degeneracy are negligible.

The following definitions and equations were used for constructing the models. Subscripts: $i =$ Region interior to the shell; $e =$ envelope; $c =$ center; $1 =$ interface between envelope and core at the shell; and $s =$ point of switch from Kramers' opacity to electron scattering.

Nondimensional variables:

$$P = p \frac{GM^2}{4\pi R^4}, \qquad T = t \frac{\mu_e H}{k} \frac{GM}{R}, \qquad M_r = qM, \qquad r = xR. \tag{1}$$

Transformation for core equations:

$$p = p_c p^*, \qquad t = t_c t^*, \qquad q = \frac{t_c^2}{l_i^2 \sqrt{p_c}} q^*, \qquad x = \frac{t_c}{\sqrt{p_c} l_i} x^*. \tag{2}$$

Absorption coefficient:

Kramers' region:

$$\kappa = \kappa_0 \frac{\rho}{T^{3.5}} \quad \text{with} \quad \kappa_0 = \frac{4 \times 10^{25}}{(t/\bar{g})} Z(1+X) \cdot \tag{3}$$

Electron-scattering region:

$$\kappa = \kappa_0 \frac{\rho_s}{T_s^{3.5}}. \tag{4}$$

Eigenvalue parameters:

Envelope:

$$C = \frac{3\kappa_0}{4ac} \left(\frac{k}{\mu_e HG}\right)^{7.5} \left(\frac{1}{4\pi}\right)^3 \frac{LR^{0.5}}{M^{5.5}}; \tag{5}$$

Core:

$$C^* = \frac{C}{q_1} j_1 \frac{L_g}{L} \frac{p_s}{t_s^{4.5}} \frac{p_c}{t_c^4}. \tag{6}$$

Composition parameters:

$$l_i = \frac{\mu_i}{\mu_e} = \frac{2X_e + \frac{3}{4} Y_e + \frac{1}{2} Z_e}{2X_i + \frac{3}{4} Y_i + \frac{1}{2} Z_i} = 2.0, \qquad j_i = \frac{Z_i (1+X_i)}{Z_e (1+X_e)} \frac{\mu_i}{\mu_e} = 1.253. \tag{7}$$

Differential equations:

Radiative envelope:

$$\frac{dp}{dx}=-\frac{pq}{tx^2}\,; \qquad \frac{dq}{dx}=\frac{x^2p}{t}\,; \tag{8}$$

$$\frac{dt}{dx}=-\frac{Cp^2}{t^{8.5}x^2} \text{ in Kramers' region ;} \tag{9}$$

$$\frac{dt}{dx}=-C\frac{p_s}{t_s^{4.5}}\frac{p}{t^4x^2} \text{ in electron-scattering region .} \tag{10}$$

Contracting core:

$$\frac{dp^*}{dx^*}=-\frac{p^*q^*}{t^*x^{*2}}\,; \qquad \frac{dq^*}{dx^*}=\frac{x^{*2}p^*}{t^*}\,; \qquad \frac{dt^*}{dx^*}=-\frac{C^*q^*p^*}{t^{*4}x^{*2}}\,. \tag{11}$$

Homology invariants:

$$U=\frac{lpx^3}{tq}\,, \qquad V=\frac{lq}{tx}\,, \qquad \text{where} \qquad l_e=1 \qquad \text{and} \qquad l_i=2\,; \tag{12}$$

$$(n+1)_e=\frac{t_s^{4.5}}{p_s}\frac{qt^4}{Cp}\,; \qquad (n+1)_i=\frac{t^{*4}}{C^*p^*}=\frac{t_s^{4.5}}{p_s}\frac{q_1}{Cj_i}\frac{L}{L_g}\frac{t^4}{p}\,. \tag{13}$$

Fitting conditions at the discontinuity:

$$\frac{U_{1i}}{U_{1e}}=\frac{V_{1i}}{V_{1e}}=l_i=2.0\,, \tag{14}$$

$$\frac{(n+1)_{1i}}{(n+1)_{1e}}=\frac{1}{j_i}\frac{L}{L_g}\,. \tag{15}$$

Density in nondimensional variables:

$$\rho=\frac{\mu}{\mu_e}\frac{p}{t}\frac{M}{4\pi R^3}\,. \tag{16}$$

III. GRAVITATIONAL ENERGY RELEASE AND THE EVOLUTIONARY FITTING CONDITION

To follow the quasi-static equilibrium states during the evolution, it is necessary to know how much energy is released by the gravitational contraction, since we must be able to apply the fitting condition equation (15). The ratio of the total luminosity to the gravitational luminosity is derived in this section.

The energy released by the core contraction in each step of the evolution is composed of three parts: (1) the change in the gravitational energy of the core between the initial and final configuration; (2) the change in the internal heat content of the core; and (3) the work, PdV, done on the core. An additional apparent source of energy must also be considered. Since the amount of mass in the core is continuously increasing as the shell exhausts its hydrogen and burns outward, additional mass is present in the final contracted state which was not present in the initial state. The additional energy due to this increment of mass, δM_1, carried into the core through the expanding interface must be subtracted from the total energy difference between the initial and final states to give the net contractional energy release. Accordingly, the net released energy as a result of contraction is

$$\bar{L}_g \delta \tau = \delta \Big[- \int_0^{r_1} \Big(C_v T - \frac{G M_r}{r} \Big) 4\pi r^2 \rho \, d r \Big] - 4\pi r_1^2 P_1 \Big(\delta r_1 - \frac{d r}{d M_r} \Big|_{r_1} \delta M_{r_1} \Big) + \Big(C_v T_1 - \frac{G M_{r_1}}{r_1} \Big) \delta M_1 . \tag{17}$$

The specific heat, C_v, is given by $C_v = k/(\gamma - 1)\mu H$. The value of γ is assumed to be $\frac{5}{3}$. To apply equation (17), it is convenient to express it in the nondimensional variables of equation (1). After some reduction, the result is

$$\bar{L}_g \delta \tau = \frac{M k T_1}{\mu_i H} \Big\{ \delta q_1 \Big(\frac{3\gamma - 4}{\gamma - 1} B_1^* + \frac{\gamma}{\gamma - 1} - U_1^* - V_1^* \Big) + q_1 \Big(\frac{3\gamma - 4}{\gamma - 1} \delta B_1^* - \frac{1}{x_1^*} \delta [U_1^* x_1^*] \Big) \Big\} , \tag{18}$$

where

$$B_1^* = \frac{1}{t_1^* q_1^*} \int_0^{x_1^*} x^{*2} p^* d x^* . \tag{19}$$

The increment of mass δM_1 carried through the expanding interface is the mass which was burned as the shell moved outward. It then follows that the nuclear energy, released simultaneously with the gravitational energy, is

$$\bar{L}_n \delta \tau = 0.007 \, c^2 X_e \delta M_1 = 0.007 \, c^2 X_e M \delta q_1 . \tag{20}$$

The ratio of equation (18) to equation (20) gives the quantity needed for the fitting condition on $n + 1$ of equation (15). With $L = L_g + L_n$, one obtains

$$\frac{\bar{L}}{\bar{L}_g} = 1 + \frac{0.007 \, c^2 X_e}{(k T_1 / \mu_i H) \{ 1.5 B_1^* + 2.5 - U_1^* - V_1^* + (q_1 / \delta q_1)(1.5 \, \delta [B_1^*] - [1/x_1^*] \, \delta [U_1^* x_1^*]) \}} . \tag{21}$$

Hence, for any proposed evolutionary change from an initial stellar state with a known temperature, pressure, and mass distribution to a known final state, the value of the right side of equation (21) may be computed. The value of $\bar{L}/\bar{L}_g$ thus obtained must agree with the mean value of L/L_g obtained from equation (15) for the initial and final states of the evolution step considered. This condition makes it possible—within the present approximations—to determine uniquely the transition states in the evolution from a given initial configuration. In the next section this evolutionary track is followed for a star whose initial configuration has an isothermal core which contains the Schönberg-Chandrasekhar limiting mass.

IV. THE CONSTRUCTION OF THE MODELS

To construct the models, a family of solutions of equations (8)–(10) for the envelope and a family of solutions of equations (11) for the core are needed. Both sets of solutions are one-parameter families in terms of the eigenvalues C and C^* as long as the appropriate absorption law is given.

The solutions to the envelope equations were obtained as follows. From Paper I of this series[1] envelope solutions of equations (8) and (9), valid for Kramers' law of opacity, were available. On the basis of trial models it became apparent, however, that, for the circumstances of interest here, electron scattering provides the main source of opacity in the inner portions of the envelopes. Accordingly, with the help of the trial models, the point where electron scattering becomes dominant was estimated for each envelope solution, and the solutions were carried from these points inward with equations (8) and (10) by numerical integration.[3] The Kramers envelope with the electron-scattering extensions are shown as heavy solid curves in Figure 1 plotted with the homology invariants U and V as co-ordinates. The electron-scattering extensions converge to the point $U = 0$, $V = 4$, which is unlike the complete Kramers envelopes that curl about $U = 1/11$, $V = 42/11$.

The one-parameter family of solutions for equation (11) of the core was obtained by numerical integration.[3] A power-series solution of equations (11) valid near the center provided starting values for the integrations. The core solutions are shown as broken curves in Figure 1.

To find the evolutionary sequence here considered, it remains only to assemble the individual models by fitting each core solution to an appropriate envelope solution by equations (14), (15), and (21). To apply equation (21), the value of B_1^* must be known. This was found along each of the seven core solutions by an elementary quadrature of equation (19). Since equation (21) connects two neighboring models in the evolutionary sequence, the individual models cannot be determined separately but must be derived successively—in the same sequence in which the star evolves through them.

To start with, the initial state has to be chosen, which—in accordance with the discussion in Section I—was here taken to be the Schönberg-Chandrasekhar limiting case for a model with an isothermal core. This initial state, represented by model I, is shown in the U-V plane of Figure 1 by the straight line (marked by I) showing the jump from (U_{1e}, V_{1e}) to (U_{1i}, V_{1i}) at the envelope-core interface.

To derive in a definite manner the next state in the evolution (to be represented by model II), a time interval for the evolution from model I to model II has to be chosen, not too long so that the changes are not too radical for the difference equation (21) to hold. Instead of choosing explicitly the time interval, the condition was here chosen so that the core of model II should correspond to $C^* = 0.200$, a value for which the core solution (see Fig. 1) does not lie too far from the core solution of model I ($C^* = 0$). Correspondingly, the point (U_{1i}, V_{1i}) for model II must lie on the core solution for $C^* = 0.200$. Choosing an arbitrary point on this solution as a trial for (U_{1i}, V_{1i}), one can read from the numerical tabulation of this solution $(n + 1)_{1i}$ needed for equation (15) and all the asterisked quantities needed for equation (21). Similarly, the point (U_{1e}, V_{1e}) corresponding to the trial for (U_{1i}, V_{1i}) can be obtained from conditions (14), and, at this point, $(n + 1)_{1e}$ and q_1 can be found by interpolation between the envelope solutions. Now all the necessary quantities are known to test the compatibility of equations (15) and (21). From equation (15) L/L_g for model II is obtained; since this quantity is already known for model I, the mean (geometrical) can be formed. From equation (21) one gets $\bar{L}/\bar{L}_g$ by using for δq_1, δB_1^*, and $\delta(U_1^* x_1^*)$ the corresponding differences between models I and II and by using for T_1, X_e, and μ_i the values assumed in Section II. If the results from the two equations do not agree, the trial point (U_{1i}, V_{1i}) must be changed—along the definite core solution—until agreement is reached. Thus unique values for U_{1i} and V_{1i} (and, in consequence, for all the other nondimensional characteristics) are found for model II. The same procedure leads from model II to model III, and so on through the entire evolution considered.

The model sequence thus obtained is precisely defined by the assumptions made in Section II. It must be remembered, however, that some of these assumptions were quite

[3] To appear in a forthcoming *Contribution of the Princeton University Observatory.*

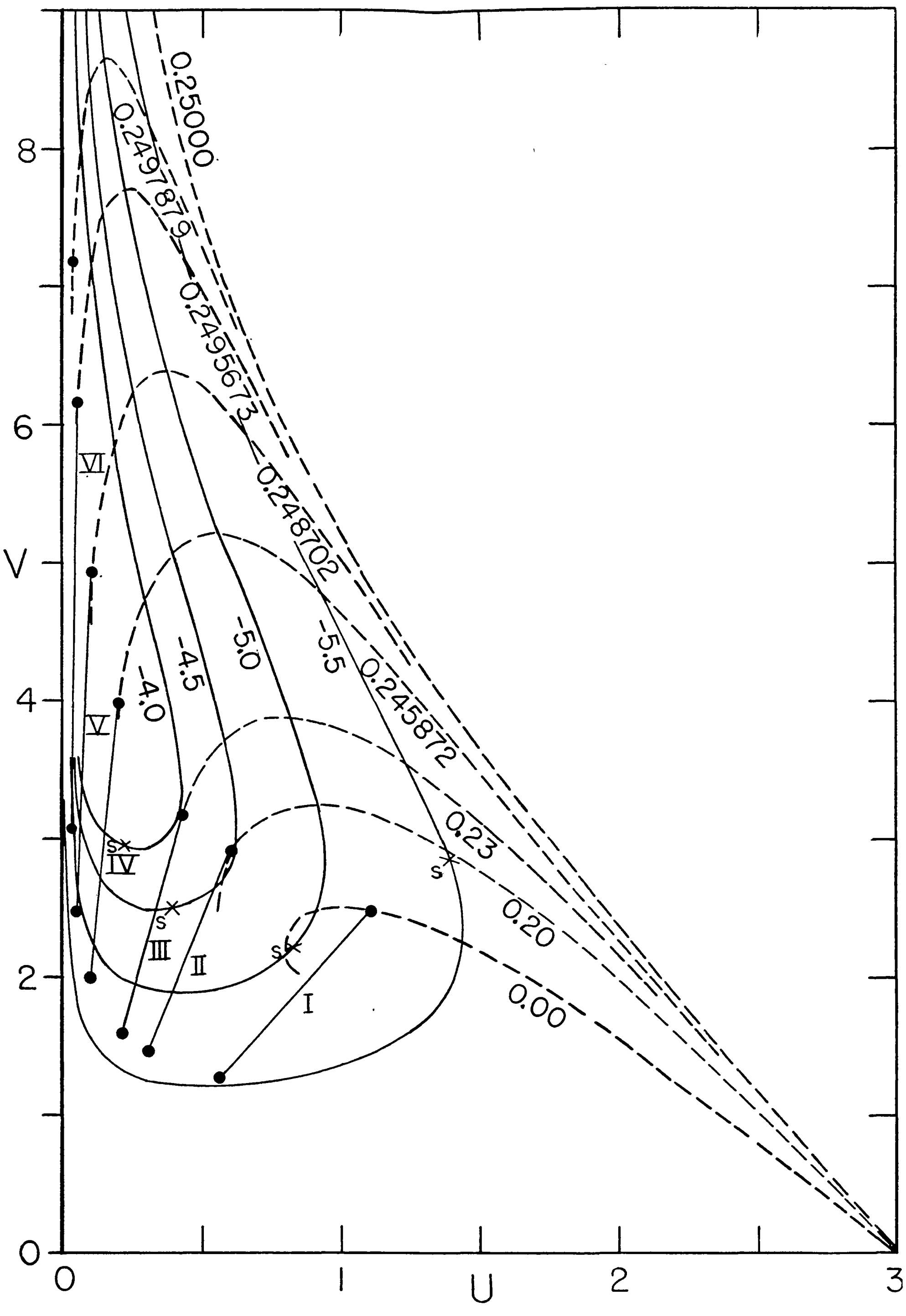

FIG. 1.—The core and envelope solutions in the U, V-plane. The heavy solid curves are envelope solutions, with their values of log C marked. Crosses marked S on the envelope solutions show the switch point from Kramers' opacity to electron scattering. The dashed curves are core solutions, with their C^* values marked. The fitting points between envelope and core for the assembled models are indicated by dots. Roman numerals on the straight connecting lines indicate the model number.

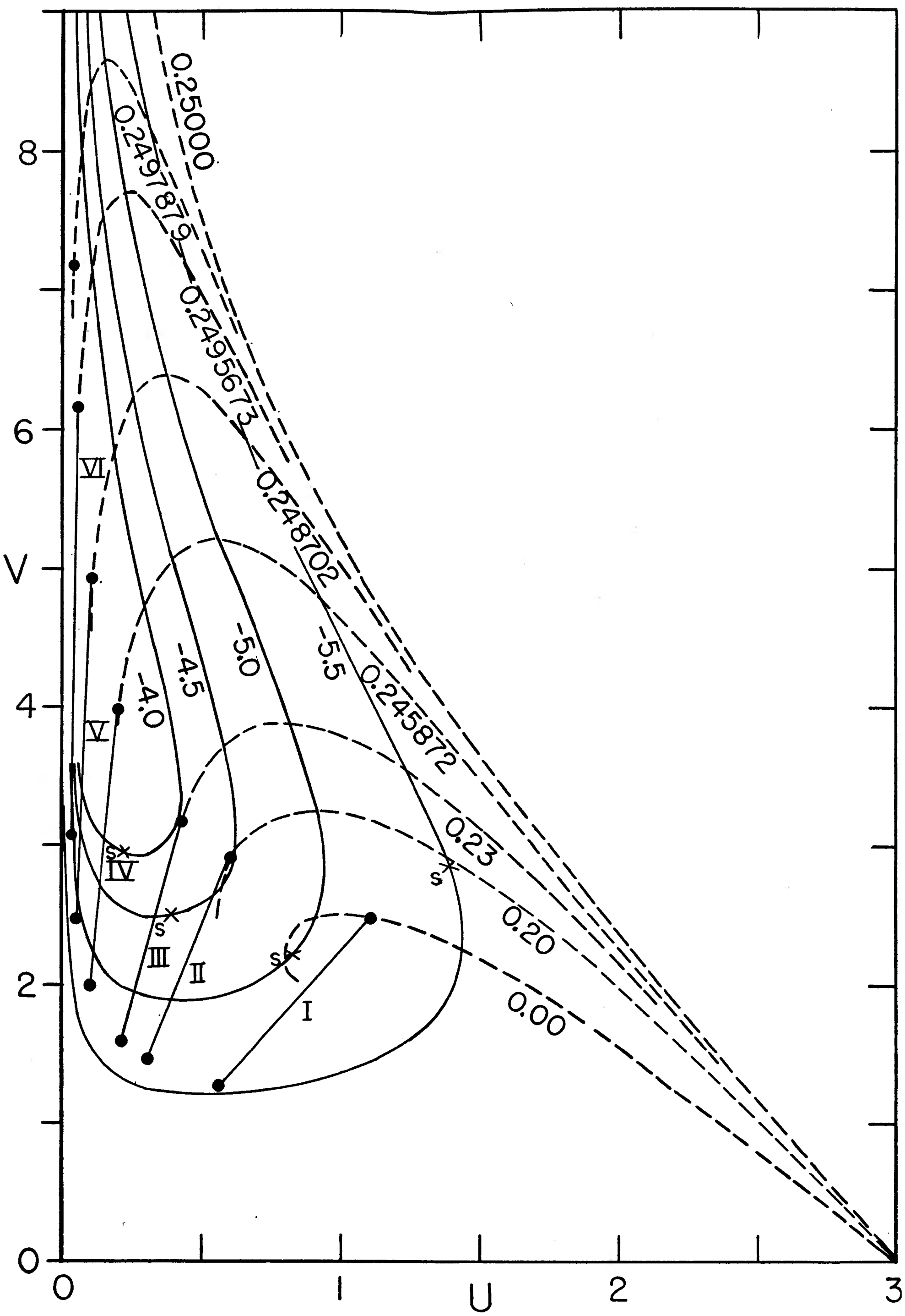

FIG. 1.—The core and envelope solutions in the U, V-plane. The heavy solid curves are envelope solutions, with their values of log C marked. Crosses marked S on the envelope solutions show the switch point from Kramers' opacity to electron scattering. The dashed curves are core solutions, with their C^* values marked. The fitting points between envelope and core for the assembled models are indicated by dots. Roman numerals on the straight connecting lines indicate the model number.

arbitrary, such as the value of 2.0 for the jump in the mean molecular weight, the assumption for the distribution of the gravitational energy sources, and the assumption of no mixing within the star.

The mathematical characteristics of the seven models shown in Figure 1 are exhibited in Table 1.

V. PHYSICAL PROPERTIES OF THE MODELS

Table 1 includes several quantities of physical interest which are independent of the mass or luminosity of the stars to which the models may be applied. The first of these quantities is log C. This parameter increases somewhat from model I to model VII but never differs greatly from its value for the corresponding Cowling model ($\log C = -6.0$). Since C is, by its definition (5), the numerical coefficient of the mass-luminosity law, it follows that stars built according to the present models follow closely the mass-luminosity

TABLE 1

MATHEMATICAL CHARACTERISTICS OF MODELS

	I	II	III	IV	V	VI	VII
U_e	0.558	0.303	0.213	0.098	0.050	0.025	0.016
V_e	1.245	1.453	1.597	1.986	2.465	3.078	3.599
C^*	0.00	0.200	0.230	0.245872	0.248702	0.2495673	0.2497879
$\log C$	−5.490	− 5.358	− 5.307	− 5.240	− 5.172	− 5.121	− 5.058
$\log p_1$	2.590	2.960	3.182	3.705	4.370	5.460	7.332
$\log t_1$	0.182	0.294	0.360	0.508	0.680	0.964	1.430
$\log t_c$	0.182	0.466	0.630	0.949	1.246	1.646	2.184
$\log p_c$	3.884	5.059	5.701	6.865	8.008	9.557	11.692
$(n+1)_e$	2.52	2.95	3.12	3.53	3.80	3.95	3.98
$(n+1)_i$	∞	148	118	101	95.1	93.4	88.0
B_1^*	1.000	1.119	1.256	1.676	2.181	2.824	3.329
L/L_g	∞	62.7	47.4	36.0	31.4	29.6	27.7
$X_1=r_1/R$	0.0643	0.0462	0.0341	0.0200	0.0109	0.0047	0.0014
$q_1=M_1/M$	0.1200	0.1232	0.1244	0.1260	0.1278	0.1298	0.1313
$\log \rho_c/\bar{\rho}$	3.526	4.418	4.893	5.739	6.587	7.734	9.333

relation of main-sequence stars—contrary to previous red-giant models, which gave overluminous stars compared to main-sequence stars of the same mass.

Next, the values of $\rho_c/\bar{\rho}$ given in Table 1 show a very large increase from model I to model VII, which represents an exceedingly great change in the structure of the star. The same is shown by the steeply decreasing values of r_1/R, which gives the fraction of the radius occupied by the exhausted core.

Finally, the large values of L/L_g indicate that, throughout the evolution here considered, at most 4 per cent of the total luminosity is provided by gravitational-energy release. Hence, even a rather small gravitational-energy source, if situated in an exhausted core, may thoroughly alter the stellar structure.

To derive the other physical characteristics, such as the radius, bolometric magnitude, and effective temperatures, the models must be applied to stars with definite values of the mass and the guillotine factor. The seven models, together with the Cowling main-sequence model,[4] were applied to stars with 1, 2, and 4 solar masses. The guillotine factor was determined by fitting Morse's[5] opacity values with the Russell mixture to the run of temperature and density of model V for a mass of $2M_{\odot}$. The coefficient κ_0 in equation (3) was adopted as $\kappa_0 = 7 \times 10^{23}$ from this fit. This corresponds to a guillotine factor of $t/\bar{g} = 1.8$.

[4] T. G. Cowling, *M.N.*, **96**, 42, 1935.

[5] P. M. Morse, *Ap. J.*, **92**, 27, 1940.

With these values for the mass and opacity coefficient, the physical characteristics shown in Table 2 were computed in the following manner.

First, the radius of the star was obtained from the second of equations (1) by applying the equation at the shell with $T_1 = 3 \times 10^7$ ° K as assumed in Section II and t_1 given by the sixth row of Table 1. The absolute bolometric magnitude was next found by solving equation (5) for the luminosity L, using the value of log C of the fourth row in Table 1. The effective temperature follows from its definition in terms of the radius and luminosity.

TABLE 2

PHYSICAL CHARACTERISTICS OF THE MODELS

	Main Sequence	I	II	III	IV	V	VI	VII
	$M/M_\odot = 1.0$							
$R/R_\odot$	0.465	0.785	1.017	1.184	1.665	2.474	4.756	13.92
M_{bol}	5.22	4.27	4.09	4.04	4.06	4.10	4.33	4.75
T_e	7,350	7,060	6,460	6,050	5,090	4,130	2,830	1,500
$T_c \times 10^{-6}$	30	30	45	56	83	110	144	170
log ρ_c	2.699	3.991	4.545	4.825	5.226	5.556	5.854	6.051
log ρ_{1i}	2.544	2.697	2.618	2.576	2.506	2.484	2.439	2.445
	$M/M_\odot = 2$							
$R/R_\odot$	0.931	1.570	2.035	2.368	3.330	4.949	9.512	27.84
M_{bol}	1.46	0.51	0.33	0.28	0.29	0.34	0.56	0.99
T_e ° K	12,300	11,900	10,900	10,200	8,570	6,950	4,760	2,520
$T_c \times 10^{-6}$ ° K	30	30	45	56	83	110	144	170
log ρ_c	2.097	3.389	3.942	4.223	4.624	4.953	5.252	5.449
log ρ_{1i}	1.942	2.095	2.015	1.974	1.904	1.881	1.837	1.843
	$M/M_\odot = 4$							
$R/R_\odot$	1.861	3.140	4.070	4.736	6.660	9.898	19.02	55.67
M_{bol}	−2.30	−3.26	−3.44	−3.48	−3.47	−3.43	− 3.20	− 2.78
T_e	20,700	20,000	18,300	17,100	14,400	11,700	8,020	4,240
$T_c \times 10^{-6}$	30	30	45	56	83	110	144	170
log ρ_c	1.495	2.787	3.340	3.622	4.024	4.352	4.650	4.847
log ρ_{1i}	1.340	1.493	1.413	1.373	1.304	1.280	1.235	1.241

The central temperature was next computed by noting from the second of equations (1) that $T_c = T_1(t_c/t_1)$. The sixth and seventh rows of Table 1 then give the central temperature. Log ρ_{1i} and log ρ_c follow immediately from equation (16) and the values in the fifth, sixth, seventh, and eighth rows of Table 1.

The results are shown in Table 2. First, it is seen that large radii characteristic of giant stars are obtained simultaneously with internal temperatures high enough for the nuclear processes to exist. Indeed, if the evolution is followed beyond model VII on the present assumptions, excessively large radii are reached.

Second, it appears to be characteristic of stars evolving along this sequence that as the core contracts, the envelope greatly expands. The details of this core contraction and envelope expansion can indeed be computed, since for each model the integrations give the fractional mass and radius distribution. Figure 2 shows the results of this computation for a mass of $2M_{\odot}$. The abscissa is the radial distance for surfaces of constant mass, in units of the solar radius. The ordinate is a time scale, whose zero epoch is at model I, derived from the rate at which q_1 increases (fourteenth row, Table 1) by the burning of the shell. The numbers at the top in Figure 2 identify the fraction, in per cent, of the total mass interior to the shell considered. Figure 2 explicitly shows the contraction of the inner shells and the expansion of the envelope layers. The star must pump energy into the expansion of the outer layers so as to overcome the gravitational potential. This energy is supplied by the outgoing flux produced by the nuclear and gravitational sources closer in. The outgoing flux is then not strictly constant in the envelope, as is assumed in equations (9) and (10) but is a decreasing function of x. This has not been taken into account in the present approximation; but this refinement is virtually certain to change the models only slightly.

Third, Table 2 shows a sharp rise in the central temperature from 3×10^7 ° K in model I to 1.7×10^8 ° K in model VII as the core contracts. The reason, of course, is that only part of the contractional energy is released as radiation flux, while the re-

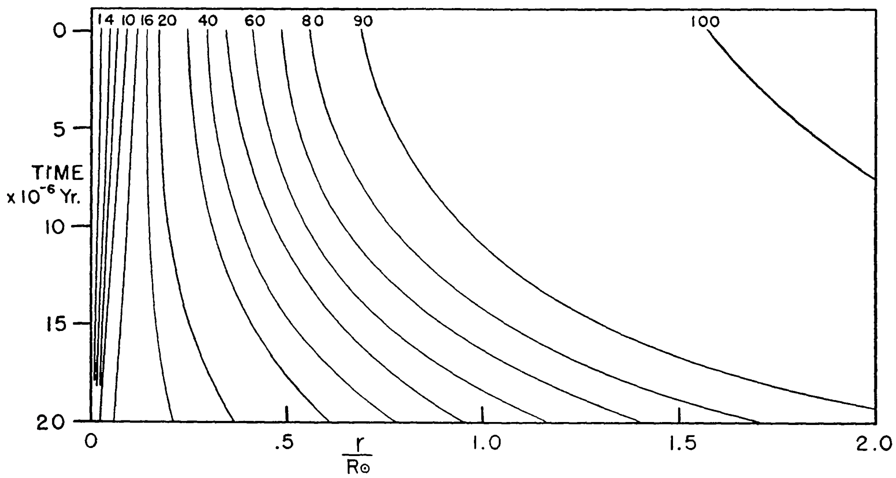

FIG. 2.—Motion of mass shells during the core contraction. Numbers at the top give the fraction of the mass, in per cent, interior to the shell considered. The abscissa is the radial distance from the center to the particular shell in units of the solar radius. The ordinate is the evolutionary time with the zero epoch at model I.

mainder goes to increase the internal energy. To illustrate the very great difference in the internal structure of models I and VII, Table 3 shows their distribution of mass, density, and temperature.

With the physical parameters for the models now known, it is possible to check certain of the assumptions of Section II. Model V with a mass of $2M_{\odot}$ was used for these checks; this is the same model to which the opacity coefficient was fitted.

The first check concerns the value of the shell temperature. If the assumed value of 30 million degrees is correct, an integration of the energy-generation equation[6] for this shell temperature must give the correct luminosity ($M_{\text{bol}} = 0.34$ model V, mass 2). Computation indicates that 28 million degrees at the shell would have given the exact required absolute magnitude and therefore that the 30-million-degree approximation is a very good one. This integration further indicated that the energy-producing shell is exceedingly narrow; the part producing 90 per cent of the energy occupies only 0.4 per cent of the radius. The idealization of representing the shell as an infinitely thin sheet therefore seems a valid one.

The second check concerns the opacity formulae (3) and (4) used in constructing the models. Equation (3) was found to represent satisfactorily the opacity in the part of the

[6] I. Epstein, *Ap. J.*, **112**, 207, 1950.

envelope outside the switching point. Equation (4), which is used to represent electron scattering in the inner parts of the models, gives a constant opacity, the value of which is chosen so as to make the absorption coefficient continuous across the switching point. This choice has the great practical advantage of making homology transformations applicable to the models. It has, however, the disadvantage that the value given by equation (4) depends strongly on the choice of the switching point, which, for best representation of the absorption coefficient, should be chosen differently for different masses (as has not been done here). Thus it is found for model V that equation (4) well represents electron scattering for stars of 4 solar masses but gives about three times too high an opacity for 2 solar masses. This malrepresentation for the lower masses appears, however,

TABLE 3

MARCH OF THE PHYSICAL VARIABLES IN MODELS I AND VII FOR $M/M_{\odot}=2$

r/R	Model I			Model VII		
	$M(r)/M$	$\log T$	$\log \rho$	M_r/M	$\log T$	$\log \rho$
0.000....	0.000	7.48	+3.39	0.000	8.23	+5.45
.005....	0.001	7.48	+3.38	0.135	7.00	+0.15
.010....	0.004	7.48	+3.30	0.140	6.77	−0.50
.015....	0.009	7.48	+3.20	0.145	6.66	−0.82
.02.....	0.019	7.48	+3.09	0.150	6.59	−1.00
.03.....	0.040	7.48	+2.85	0.160	6.49	−1.22
.04.....	0.064	7.48	+2.61	0.172	6.42	−1.39
.05.....	0.084	7.48	+2.40	0.185	6.37	−1.50
.06.....	0.102	7.47	+2.14	0.200	6.32	−1.61
.07.....	0.120	7.45	+1.78	0.220	6.28	−1.70
.08.....	0.138	7.43	+1.72	0.240	6.25	−1.79
.09.....	0.156	7.41	+1.69	0.260	6.22	−1.84
.10.....	0.175	7.38	+1.63	0.290	6.18	−1.92
.15.....	0.285	7.27	+1.46	0.445	6.07	−2.30
.20.....	0.417	7 18	+1.25	0.580	5.97	−2.58
.25.....	0 555	7.08	+1.02	0.704	5.87	−2.88
.30.....	0.686	7.00	+0.80	0.800	5.78	−3.12
.40.....	0.849	6.83	+0.31	0.910	5.59	−3.60
.50.....	0.935	6.67	−0.19	0.975	5.42	−4.15
.60.....	0.975	6.49	−0.74	1.00	5.24	−4.75
.70.....	0.992	6.30	−1.40	1.00	5.07	−5.39
.80.....	0.998	6.06	−2.12	1.00	4.82	−6.12
0.90.....	1.00	5.70	−3.31	1.00	4.47	−7.30

to have very little effect on the models, as was shown by test models in which Kramers' absorption law was used throughout. Even though the opacity in the inner portions of these models was too small by a large factor, the test models differed little from the final ones. Hence it is not expected that the present models would be much changed by an improved representation of the absorption coefficient.

The third check concerns the neglect of radiation pressure. In the most unfavorable case, that of model VII with a mass of $4M_{\odot}$, the ratio of the total pressure to radiation pressure at the interface of the core and envelope is 20 to 1, while at the center this ratio becomes 490 to 1, indicating that for the range of masses here considered radiation pressure plays virtually no role.

The fourth and final check concerns the assumption for the neglect of degeneracy. The values in the fourth and fifth rows of Table 2 plotted in the degeneracy diagram of G. Wares[7] shows that models of mass $1M_{\odot}$ are all slightly degenerate at their centers.

[7] *Ap. J.*, **100**, 158, 1944.

The centers of mass $4M_{\odot}$ models are practically on the degeneracy criterion line. Since the degeneracy is very slight and is confined to the central region of the cores, the general features of the models based upon the assumption of no degeneracy should be quite generally valid.

One additional check on the assumptions is possible concerning the distribution of the gravitational-energy sources. Since the distribution of mass is known for the completed models, it is possible to compute the change of the gravitational potential from one contractional state to the next and check the assumption of ϵ = constant. This has not been

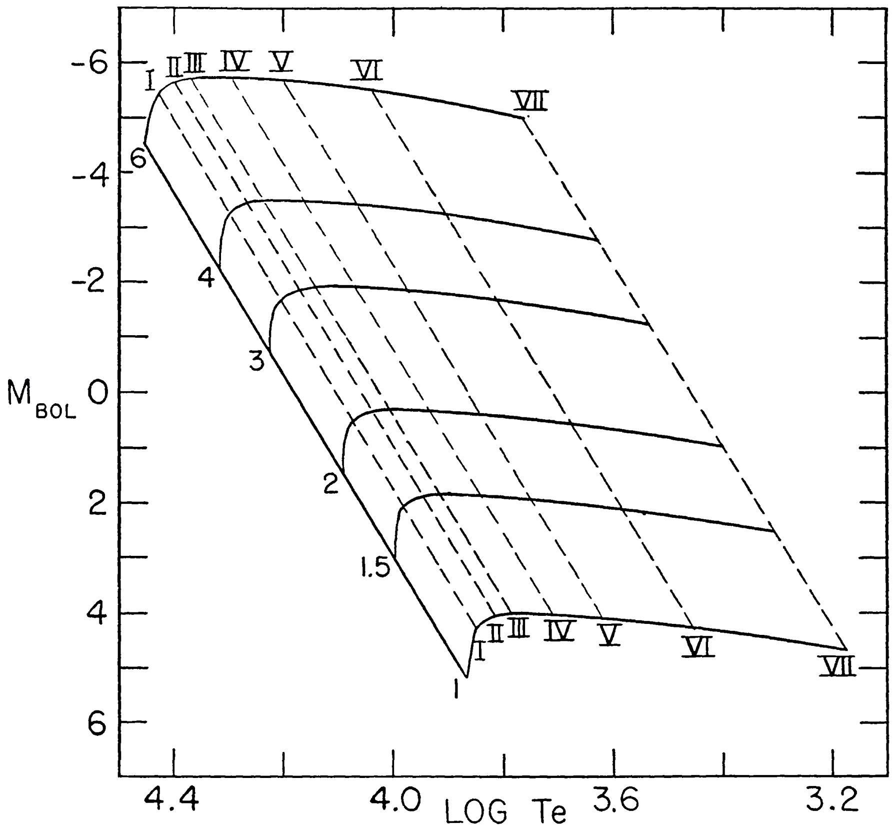

FIG. 3.—The evolutionary tracks in the H–R diagram. Each of the heavy curves gives the line of evolution for star of a given mass, the value of the mass being given at the left of the curve. The intersections of the dashed and solid lines are the positions of models I–VII for the various masses. The straight line to the left represents the main-sequence Cowling model.

done, but estimates indicate that the models are rather insensitive to the exact distribution of sources assumed.

All indications then seem to be that the models here presented are consistent with the assumptions used in deriving them.

VI. THE EVOLUTIONARY TRACK IN THE H-R DIAGRAM AND THE AGE OF GLOBULAR CLUSTERS

Figure 3 shows the evolutionary tracks in the H-R plane from the data of Table 2. This diagram summarizes the evolutionary path taken by stars of various masses during the time that their cores are contracting. No attempt has been made to fit the observational data for the main sequence.

As Schönberg and Chandrasekhar[2] first pointed out, the star increases slightly in luminosity in going from the main sequence to model I, becoming about 1 mag. brighter when the 12 per cent limit for the exhausted mass is reached at model I. At this point $R = 1.7\ R_{\text{Cowling}}$, while the effective temperature has remained nearly constant. Thus, from the Cowling model to the limiting isothermal core model, the stars remain in the vicinity of the main sequence. The contraction of the core—with its consequent envelope expansion—begins with model I, and the stars rapidly move away from the main sequence into the giant region.

Figure 3 suggests the following phenomenon for the Hertzsprung-Russell diagram for old stellar systems—such as globular clusters—in which all stars are presumably of the same age. The fainter stars of such a system will not yet have burned up 12 per cent of their mass and will therefore be on or near the main sequence. The brighter stars will have burned up more than 12 per cent of their mass and will therefore—under the present assumptions—have moved to the right in the H-R diagram. According to Figure 3, the evolution to the right sets in rather sharply for any given star. Hence one should expect a fairly well-defined turnoff point in the H-R diagrams of these systems, as has indeed been observed.[8] The stars at the turnoff point should then be identified with those which have just reached the Schönberg-Chandrasekhar limit, i.e., have just burned out 12 per cent of their mass.

If this identification is correct, one may theoretically compute the absolute magnitude at which the turnoff point should occur in a system of an age of, say, $t = 3 \times 10^9$ years. For stars which have burned out q_1 per cent of their mass, one has

$$L\tau = 0.007\, c^2 X_e q_1 M\ . \tag{22}$$

Combining this with the appropriate mass-luminosity relation and using, as before, $X_e = 0.596$ and $q_1 = 12$ per cent, one gets a mass of 1.3 solar masses and a luminosity corresponding to $M_{\text{bol}} \approx +3.3$. (This result is fairly independent of the assumed hydrogen content, X_e, since, for varying X_e also, the jump of the molecular weight at the discontinuity varies. In consequence, the core-mass fraction q_1 of the Schönberg-Chandrasekhar limit varies[9] in such a way that the product $X_e\, q_1$ occurring in eq. [22] remains nearly constant.)

On the observational side, the turnoff point in M 92 and M 3 is found at $M_{\text{bol}} = +3.6$. The agreement between the computed and observed values appears so good that it may fairly be taken as a confirmation of the above interpretation of the observed turnoff point.

Inverting the argument, one may also take this agreement as indicating the correctness of the assumed age of the globular clusters, at least within a factor of 2.

VII. SPECULATION ON THE BRIGHTER STARS IN GLOBULAR CLUSTERS

In the previous section we have discussed the early evolutionary phases of unmixed stars, from the Cowling model through the Schönberg-Chandrasekhar limit to the beginning of the core contraction with simultaneous envelope expansion. It is tempting now to speculate on the subsequent evolutionary phases which presumably are represented by the brighter globular cluster stars which may have gone through the earlier phases at a relatively faster rate, owing to a somewhat larger mass. However, for these subsequent phases the present models are soon found quite inadequate, and only some qualitative estimates seem possible until further integrations are made.

The first difficulty arises when the rate is computed with which a star evolves from model I to model VII. By using equation (22) (but replacing L by L_n and q_1 by δq_1), one finds that a star evolves from model I to model VII in about a twentieth of the time it takes to evolve from the Cowling model to model I. Hence one should expect in the H-R

[8] Arp, Baum, and Sandage, *A.J.*, **57**, 4, 1952.

[9] Harrison, *Ap. J.*, **105**, 322, 1947.

diagram of a globular cluster a good deal fewer stars just beyond the Schönberg-Chandrasekhar limit (model I) than just below this limit contrary to observation. Preliminary tests, however, seem to indicate that the evolution rate during the core contraction may possibly be appreciably modified by moderate changes in the present assumptions, so that this difficulty, though not solved, does not seem too serious.

A second difficulty arises when the extent of the envelope expansion is considered. Under the present assumptions there is no reason why the envelope expansion should stop at or before model VII, while the observed H-R diagrams of globular clusters seem to indicate that the expansion should essentially stop about at model V, and then mainly a brightening (increase in C) and only little further expansion (little increase in t_1) should occur. One may speculate that around model V a physical process not included in the present computations should start to play an essential role.

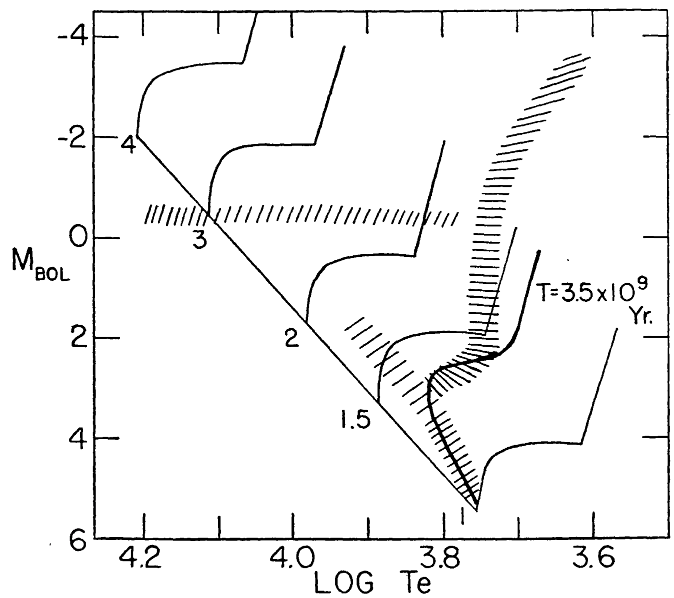

FIG. 4.—Speculative evolutionary tracks for stars of various masses with an assumed temperature of 1.1×10^8 ° K for the helium burning. The schematic globular cluster H–R diagram is shown for comparison. The heavy line is the theoretical appearance of the diagram 3.5×10^9 years after the formation of the stars.

As a first hypothesis for the needed process, one may think of the transmutation of helium into heavier elements. The central temperature reached in model V (1.1×10^8 ° K) is rather lower than the temperature needed for helium burning (2×10^8 ° K) as derived by Salpeter,[10] but still just within the limits of the uncertainty of this derivation. Following this hypothesis, preliminary estimates were made for the subsequent models which should consist of a hydrogen-rich envelope, a shell in which hydrogen burns, a helium-rich intermediate zone, a shell in which helium burns, and an inert core of heavy elements. The estimated evolution through these phases is indicated in Figure 4 in the vertical upper ends of the heavy lines, with the assumption of 1.1×10^8 ° K for the temperature of the helium burning. (The main-sequence model and models I–V are not quite plotted at the same places in Figs. 3 and 4, since in the latter case shell temperatures ranging from 20×10^6 ° K for the main sequence to 30×10^6 ° K for model V were used instead of 30×10^6 ° K throughout Fig. 3.) Whenever the evolution tracks for individual stars are given in the H-R diagram, one can derive a curve

[10] E. Salpeter, *Ap. J.*, **115**, 326, 1952.

crossing the tracks and connecting all points reached by stars of various masses at the same time. Such a curve, computed for a time of 3.5×10^9 years, is shown by the heavy line in Figure 4. This curve seems to fit well the main observed feature of the lower portions of the H-R diagram of globular clusters. Nevertheless, it seems far from certain whether this hypothesis regarding the early termination of the envelope expansion is correct, since the necessary temperature for the helium burning seems rather low.

As a second hypothesis for the process causing the termination of the expansion, one might think of moderate mixing of the layers near the shell caused by rotation. This would decrease the effect of the chemical inhomogeneity and thus reduce the expansion. The mixing by rotation should affect all evolutionary phases but possibly the later ones particularly strongly. It then seems plausible that the observed feature of the H-R diagram of globular clusters might be explained by changing the present models by introducing a moderate amount of mixing. To follow this, however, further integrations are necessary.

VIII. SUMMARY

The application of the evolutionary fitting condition of Section III has made it possible to follow from an initial state the evolution of stars built on a shell-source model with a chemical discontinuity between the envelope and a contracting core. The detailed computations show that as the core contracts, liberating gravitational energy, the envelope greatly expands (Fig. 3), giving giant stars with internal temperatures high enough for the nuclear processes to provide the required luminosities.

A theoretical Hertzsprung-Russell diagram based on the derived models was compared with the observed diagrams for globular clusters. Good agreement was found for the fainter stars, i.e., the earlier evolution phases. However, the present models were found inadequate to explain the brighter features of the diagram.